PERFORMANCE INVESTIGATION AND MULTI-OBJECTIVE OPTIMIZATION OF END MILLING OF ALUMINIUM ALLOY 6061 T6 WITH COATED AND UNCOATED CARBIDE TOOLS UNDER VARIOUS COOLING CONDITIONS

SYEDA NAJIHA MASOOD

Thesis submitted in fulfilment of the requirements
for the award of the degree of
Doctor of Philosophy in Mechanical Engineering

Faculty of Mechanical Engineering
UNIVERSITI MALAYSIA PAHANG

November 2015

ABSTRACT

Application of cutting fluids as cooling and lubricating media is considered essential in manufacturing practices on account of providing lubrication, heat transfer capabilities, corrosion minimization as well as flushing away of metal chips and debris. On account of sizable costs, increasing eco-awareness, implementation of sustainability indices in manufacturing units and strict regulations due to detrimental effects of cutting fluids to the environment and the human exposure, economically viable substitutes to cutting fluids are being explored. Minimum quantity lubrication (MQL) technique offers a near-term solution to the problem. The objectives of this study are to investigate the machining performance and to develop multi-objective optimization model in end milling of aluminium alloy AA6061-T6 with conventional MQL and nanofluid-MQL techniques. Uncoated tungsten carbide (WC-Co 6.0%) and PVD TiAlN and TiAlN+TiN coated carbide cutting tools are considered using 23.4-54.0 ml/hr flow rate of commercial mineral oil for MQL machining with different combinations of input cutting parameters. Nanofluid % volume fraction is varied from 0.5 %-4.5 %. Response surface methodology (RSM) with central composite design approach is used for the design of experiments. Second order mathematical models are developed for machining performance measures with different cooling conditions and validated statistically. The developed models show good agreement (< 5 % error) with the experimental results. PVD coated carbide tools outperformed uncoated tool in terms of tool damage and surface quality and uncoated tool is selected for the nanofluid MQL machining. The effectiveness of MQL is compared with conventional flooded conditions. Nanofluid-MQL exhibits superior performance compared to flooded and conventional MQL in terms of surface roughness and tool wear. For material removal rate results are almost similar in all cases. Tool damage is characterized by SEM micrographs and EDX patterns. Adhesion, edge chipping and coating damage for uncoated and coated tools are observed with higher feed rate, higher depths of cut and lower MQL flow rate. The major benefit from the water-based nanofluid MQL is shown in the edge integrity, which is attributed to the cooling effect produced due to latent heat of vaporization of water. Experimental results show the prospective utilization of water-based TiO_2 nanofluid as MQL cooling medium. Comprehensive multi-objective optimization model using genetic algorithm is developed to optimize machining performance measures under different MQL conditions, based on Pareto optimal design approach. As a result of optimization, the resultant improvements in surface roughness and flank wear in conventional MQL machining for uncoated tungsten carbide tool are 74.2 % and 58.4 %; for PVD TiAlN coated tools are 16.9 % and 73.6 %; for PVD TiAlN+TiN coated tool are 60 % and 41.4 %, respectively. For nanofluid-MQL machining, the optimum nanofluid volume concentration is 2.64 %. Promising results of the study in terms of process performance, compared with traditional practices, highly advocate the use of MQL technique with water-based nanofluid in industrial machining application as well as academia activities.

ABSTRAK

Aplikasi bendalir pemotong sebagai medium penyejukan dan pelinciran amat penting dalam pembuatan yang melibatkan jumlah pelincir, kebolehtahanan pertukaran haba, pengurangan karat dan juga pembuangan cip logam and minyak. Disebabkan oleh faktor kos, peningkatan kesedaran-eco, perlaksanaan konsep kelestarian dalam unit pembuatan dan peraturan yang ketat berkaitan dengan kesan bendalir pemotongan terhadap persekitaran dan pendedahan kepada amanusia, secara ekonominya perlu diganti dan bendalir pemotongan perlu dikaji. Kaedah pelinciran kuantiti minimum (MQL) menawarkan penyelesaian kepada masalah ini. Objektif kajian ini adalah menyiasat persembahan pemesinan dan pembangunan model objektif optimum pelbagai dalam proses pemesinan logam aluminium AA6061-T6 dengan menggunakan MQL konvensional dan teknik MQL-bendalir-nano. Alatan pemotong tunsten karbida tanpa salutan (WC-Co 6.0%) dan karbida bersalut PVD digunakan menggunakan kadar aliran 23.4-54.0 ml/hr minyak mineral komersial untuk pemesianan MQL dengan kepelbagaian parameter masukan pemesinan. Jumlah peratusan pecahan bendalir nano dipelbagaikan dari 0.5 hingga 4.5 %. Kaedah tindakan permukaan dengan pendekatan rekabentuk komposit berpusat digunakan untuk rekabentuk eksperimen. Model matematik kedua dibangunkan untuk mengukur persembahan pemesinan dengan keadaan pelbagai penyejukan dan ditentushakan secara statistik. Model yang dibangunkan menunjukkan persetujuan yang baik (ralat kurang 5 %) dengan keputusan eksperimen. Alatan PVD bersalut karbida mengatasi persembahan alatan tidak bersalut pada kerosakan alat dan kemasan permukaan, maka alatan tidak bersalut digunakan unutk pemesinan MQL bendalir-nano. Keberkesanan MQL dibandingkan dengan keadaan keadaan konvensioanal penyejukkan banjir. Bendalir-nano MQL menunjukkan persembahan cemerlang berbanding dengan penyejukkan banjir dan konvensional MQL pada kemasan permukaan dan kehausan alatan. Untuk kadar pembuangan bahan menunjukkan keputusan yang sama bagi semua kes. Kerosakan alatan diselidiki dengan mikro geraf SEM and corak EDM. Pelekatan, serpihan sisi dan kerosakan salutan untuk alatan bersalut dan tidak bersalut diperhatikan pada kadar masukan yang tinggi dan kadar aliran MQL yang rendah. Kelebihan yang besar diperolehi dari MQL bendalir nano berasaskan air ditunjukkan pada integriti sisi, yang mana disebabkan oleh kesan penyejukkan yang terhasil daripada pemeluapan haba laten air. Keputusan eksperimen menunjukkan prospek penggunaan bendalir nano berasaskan air TiO_2 sebagai medium penyejukan MQL. Model objektif optimum pelbagai yang komprehensif menggunakan algoritma genetik dibangunkan untuk mengoptimumkan persembahan pemesinan diukur pada kelainan keadaan MQL, berasaskan kaedaan optimal rekabentuk Pareto. Hasil keputusan pengoptimuman, menunjukkan penambahan kemasan permukaan dan kehausan rusuk pada pemesinan konvensional MQL untuk alatan karbida tunsten yang tidak bersalut adalah 74.2 % dan 58.4 %; untuk alatan bersalut PVD TiAlN adalah 16.9 % dan 73.6 %; untuk alatan bersalut PVD TiAlN+TiN masing-masing adalah 60 % dan 41.4 %. Untuk pemesinan bendalir nano MQL, kepekatan isipadu bendalir nano yang optimum adalah 2.64 %. Harapan keputusan daripada kajian ini dalam persembahan proses, berbanding dengan praktikal tradisional, penggunaan kaedah MQL dengan bendalir nano berasaskan air sangat dicadangkan dalam industri aplikasi pemesinan dan juga aktiviti-aktiviti akademik.

TABLE OF CONTENTS

	Page
SUPERVISOR'S DECLARATION	ii
STUDENT'S DECLARATION	iii
DEDICATION	iv
ACKNOWLEDGEMENTS	v
ABSTRACT	vi
ABSTRAK	vii
TABLE OF CONTENTS	viii
LIST OF TABLES	xii
LIST OF FIGURES	xv
LIST OF SYMBOLS	xxii
LIST OF ABBREVIATIONS	xxv

CHAPTER 1 INTRODUCTION

1.1	Introduction	1
1.2	Problem Statement	3
1.3	Objectives of the Study	6
1.4	Scope of the Study	6
1.5	Organization of Thesis	7

CHAPTER 2 LITERATURE REVIEW

2.1	Introduction	8
2.2	Cutting Fluids in Sustainable Manufacturing	8
2.3	Sustainable Machining Systems	10
	2.3.1 Dry Machining	12
	2.3.2 High Pressure Coolant Technique	13
	2.3.3 Solid Lubricant Technique	14
	2.3.4 Air, Vapor and Gas Coolant	15
	2.3.5 Cryogenic Coolants	16
	2.3.6 Minimum Quantity Lubrication	17
2.4	Nanofluids	25

2.4.1 Nanofluids as Coolants 26
2.4.2 Nanofluids as Lubricants 27

2.5 Properties of Nanofluids 28

2.5.1 Thermal Conductivity 28
2.5.2 Convective Heat Transfer Coefficient 28
2.5.3 Viscosity of Nanofluids 30

2.6 Nanofluids in Machining Applications 32

2.7 Multi-Objective Optimization in Machining 36

2.8 Tool Wear with Aluminium and Aluminium Alloys 39

2.9 Summary 43

CHAPTER 3 EXPERIMENTAL WORK AND OPTIMIZATION MODELLING

3.1 Introduction 44

3.2 Flow Chart of the Study 44

3.3 Materials 45

3.3.1 Workpiece Material 45
3.3.2 Cutting Fluids 46
3.3.3 Cutting Tool and Inserts 48

3.4 Machining Parameters 50

3.4.1 Process Parameters 51
3.4.2 Performance Parameters 53

3.5 Experimental Details 58

3.5.1 Design of Experiments 58
3.5.2 Experimental Setup 60
3.5.3 MQL System 62

3.6 Mathematical Modelling 64

3.6.1 Model Development 64
3.6.2 Analysis of Variance 66

3.7 Preparation of Nanofluid 67

3.8 Properties of Nanofluid 69

3.8.1 Density 69
3.8.2 Thermal Conductivity Measurement 70
3.8.3 Viscosity and pH of TiO_2 Nanofluid 71

3.9 Multi-Objective Optimization 72

3.9.1 Optimization Modelling 74
3.9.5 Optimization Algorithm 76

	3.9.6 Multi-Criteria Decision Making	79
3.10	Modelling and Optimization Tools	80
3.11	Summary	81

CHAPTER 4 RESULTS AND DISCUSSION

4.1	Introduction	82
4.2	Mathematical Modelling	82
	4.2.1 Material Removal Rate	83
	4.2.2 Surface Roughness	90
	4.2.3 Flank Wear	98
4.3	Confirmation Runs	99
4.4	Effects of Input Parameters on Response Variables	101
	4.4.1 Material Removal Rate	102
	4.4.2 Surface Roughness	107
	4.4.3 Flank Wear	125
	4.4.4 Wear Maps	144
4.5	Performance Comparison	151
4.6	Wear Mechanisms	154
	4.6.1 Uncoated Tungsten Carbide Insert	154
	4.6.2 TiAlN Coated Insert	163
	4.6.3 TiAlN+TiN Coated Insert	172
	4.6.4 Energy Dispersive X-Ray Analysis	182
4.7	Tool Wear for Nanofluid-MQL Conditions	187
4.8	Surface Roughness as a Measure of Flank Wear	213
4.9	Machining Performance of the Tools	216
4.10	Optimization Performance	218
	4.10.1 Uncoated Tungsten Carbide Insert in Conventional MQL	218
	4.10.2 TiAlN Coated Insert in Conventional MQL	221
	4.10.3 TiAlN+TiN Coated Insert in Conventional MQL	224
	4.10.4 Uncoated Tungsten Carbide Insert in Nanofluid-MQL	224
4.11	Selection of Best Solutions	228
4.12	Confirmation Runs for Optimization	229
4.13	Summary	230

CHAPTER 5 CONCLUSIONS AND RECOMMENDATIONS

5.1 Introduction 232

5.2 Summary of Findings 232

5.2.1 Modelling of Machining Performance Measures 232
5.2.2 Performance Analysis 233
5.2.3 Optimization 235

5.3 Contributions of the Study 236

5.4 Recommendations for Future Work 237

REFERENCES 238

LIST OF PUBLICATIONS 264

APPENDICES

A1 Measured values of average surface roughness in flooded conditions 266

A2 Measured values of material removal rate (MRR) in flooded conditions 267

A3 Measured values of flank wear in flooded conditions 268

A4 Measured values of average surface roughness in conventional MQL conditions 269

A5 Measured values of average surface roughness with uncoated carbide insert in nanofluid MQL conditions 270

A6 Measured values of material removal rate in conventional MQL conditions 271

A7 Measured values of material removal rate with uncoated carbide insert in nanofluid-MQL conditions 272

A8 Measured values of flank wear in conventional MQL conditions 273

A9 Measured values of flank wear with uncoated carbide insert in nanofluid MQL conditions 274

LIST OF TABLES

Table No.	Title	Page
2.1	Thermal conductivity enhancement in TiO_2–water nanofluids	29
2.2	Summary of convective heat transfer properties of nanofluids	31
2.3	Volume fraction dependent viscosity of nanofluids	31
3.1	The alloy composition of the AA6061-T6	46
3.2	Physical, thermal and mechanical properties of AA6061-T6	46
3.3	Composition, properties and dimensions of end mill inserts	49
3.4	Levels assigned to the input cutting parameters for flooded, conventional MQL and nanofluid-MQL cooling	60
3.5	Specifications of the HAAS-VF6 vertical machining center	62
3.6	Measured values of viscosity and pH for different fractions of nanofluid	72
3.7	Software tools used in the research	80
4.1	Estimated regression coefficients for material removal rate with different cooling conditions for uncoated tungsten carbide insert	84
4.2	ANOVA for material removal rate with uncoated tungsten carbide insert with different cooling conditions	85
4.3	Estimated regression coefficients for material removal rate with different cooling conditions for TiAlN coated tungsten carbide insert	86
4.4	ANOVA for material removal rate with TiAlN coated tungsten carbide insert with different cooling conditions	87
4.5	Estimated regression coefficients for material removal rate with different cooling conditions for TiAlN+TiN coated tungsten carbide insert	88
4.6	ANOVA for material removal rate with TiAlN+TiN coated carbide insert with different cooling conditions	89

Table No.	Title	Page
4.7	Estimated regression coefficients for surface roughness with different cooling conditions for uncoated tungsten carbide insert	91
4.8	ANOVA for surface roughness with uncoated tungsten carbide insert	92
4.9	Estimated regression coefficients for surface roughness with different cooling conditions for TiAlN coated tungsten carbide	94
4.10	ANOVA for surface roughness with TiAlN coated tungsten carbide carbide insert	95
4.11	Estimated regression coefficients for surface roughness with different different cooling conditions for TiAlN+TiN coated tungsten carbide insert	96
4.12	ANOVA for surface roughness with TiAlN+TiN coated tungsten carbide insert	97
4.13	Coefficient of determination (R-Sq value) for flank wear models with different inserts	98
4.14	Errors of developed models for surface roughness and flank wear	100
4.15	DOE main and interaction effects of input cutting parameters on removal rate in different cooling conditions with different tools	101
4.16	DOE main and interaction effects of input cutting parameters on surface surface roughness in different cooling conditions with different tools	107
4.17	DOE main and interaction effects of input cutting parameters flank wear in different cooling conditions with different tools	128
4.18	Regression coefficients for surface roughness growth model	215
4.19	Designs of experiment for determining M-ratio in conventional -MQL MQL and nanofluid-MQL machining	216
4.20	M-ratio for uncoated and coated inserts in conventional MQL machining	217
4.21	M-ratio for uncoated tungsten carbide inserts in nanofluid-MQL machining	218

Table No.	Title	Page
4.22	Optimum cutting variables and optimum solutions	227
4.23	Errors of optimized models for surface roughness and flank wear	229

LIST OF FIGURES

Figure No.	Title	Page
3.1	Flow Chart of the Study	45
3.2	Workpiece blank and machined workpiece with dimensions in mm	47
3.3	Two-flute MaxiMill cutter	48
3.4	UW6200 top loading digital balance (Shimadzu)	54
3.5	Cutter traversed length	55
3.6	Average roughness parameter	56
3.7	HAAS CNC vertical machining center (HAAS-VF6)	61
3.8	Setup of workpiece	61
3.9	Surface roughness testers and scanning electron microscope	62
3.10	MQL System and setting	63
3.11	Preparation of TiO_2 nanofluid for different % volume fractions	68
3.12	TEM Image of TiO_2 nano-particles at 100 nm magnification	69
3.13	Effects of TiO_2 volume fraction on effective density	70
3.14	Effects of TiO_2 volume fraction on effective thermal conductivity	71
3.15	Flowchart for multi-objective optimization technique	73
3.16	Flow chart for MOGA-II algorithm	77
3.17	Pseudocodes for MOGA-II algorithm	78
4.1	Flank wear obtained from confirmation runs for conventional MQL and nanofluid-MQL conditions	100
4.2	DOE main and interaction effects Box-whiskers plots for material removal rate obtained with uncoated tungsten carbide insert with conventional MQL	103
4.3	DOE main and interaction effects Box-whiskers plots for material removal rate obtained with TiAlN coated tungsten carbide insert with conventional MQL	103

Figure No.	Title	Page
4.4	DOE main and interaction effects Box-whiskers plots for material removal rate obtained with TiAlN+TiN coated tungsten carbide insert with conventional MQL	104
4.5	DOE main and interaction effects Box-whiskers plots for material removal rate for uncoated tungsten carbide insert with nanofluid MQL	104
4.6	Significance of input parameters for material removal rate for different cutting tools with different cooling conditions	105
4.7	Variations of material removal rate against depth of cut and feed rate	106
4.8	DOE main and interaction effects Box-whiskers plots for surface roughness for uncoated tungsten carbide insert with conventional MQL	108
4.9	DOE main and interaction effects Box-whiskers plots for surface roughness for TiAlN coated tungsten carbide insert with conventional MQL	108
4.10	DOE main and interaction effects Box-whiskers plots for surface roughness for TiAlN+TiN coated tungsten carbide insert with conventional MQL	109
4.11	DOE main and interaction effects Box-whiskers plots for surface roughness for uncoated tungsten carbide insert with nanofluid-MQL	109
4.12	Significance of input parameters for surface roughness for various cutting tools with different cooling conditions	111
4.13	Variations of surface roughness against input cutting parameters with uncoated tungsten carbide insert in conventional MQL	113
4.14	Variations of surface roughness against input cutting parameters with uncoated tungsten carbide insert in nanofluid-MQL	115
4.15	Variations of surface roughness against input cutting parameters with TiAlN coated carbide insert in conventional MQL	118
4.16	Variations of surface roughness against input cutting parameters with TiAlN+TiN coated carbide insert in conventional MQL	120

Figure No.	Title	Page
4.17	DOE main and interaction effects Box-whiskers plots for flank wear obtained with uncoated tungsten carbide insert with conventional MQL	126
4.18	DOE main and interaction effects Box-whiskers plots for flank wear obtained with TiAlN coated tungsten carbide insert with conventional MQL	126
4.19	DOE main and interaction effects Box-whiskers plots for flank wear obtained with TiAlN+TiN coated tungsten carbide insert with conventional MQL	127
4.20	DOE main and interaction effects Box-whiskers plots for flank wear obtained with uncoated tungsten carbide insert with nanofluid MQL	127
4.21	Significance of input parameters for flank wear for various cutting tools with different cooling conditions	129
4.22	Variations of flank wear against input cutting parameters with uncoated tungsten carbide insert in conventional MQL	130
4.23	Variations of flank wear against input cutting parameters with TiAlN coated insert in conventional MQL	132
4.24	Variations of flank wear against input cutting parameters with TiAlN+TiN coated insert in conventional MQL	133
4.25	Variations of flank wear against input cutting parameters with uncoated tungsten carbide insert in nanofluid-MQL	135
4.26	Wear maps for uncoated tungsten carbide insert in flooded and conventional MQL	145
4.27	Wear maps for uncoated tungsten carbide insert in nanofluid-MQL machining	146
4.28	Wear maps for TiAlN coated inserts in flooded and conventional MQL	148
4.29	Wear maps for TiAlN+TiN coated inserts in flooded and conventional MQL	150
4.30	Performance comparison of three inserts in conventional MQL machining	152

Figure No.	Title	Page
4.31	SEM micrographs of uncoated tungsten carbide in conventional MQL conditions at speed=5300 RPM, feed rate = 440 mm/min, MQL flow rate = 0.83 ml/min	155
4.32	SEM micrographs of uncoated tungsten carbide in conventional MQL conditions speed=5400 RPM, feed rate = 379 mm/min, MQL flow rate = 0.65 ml/min.	157
4.33	SEM micrographs of uncoated tungsten carbide insert for conventional MQL at depth of cut = 2.0 mm	159
4.34	SEM micrographs of uncoated tungsten carbide insert for conventional MQL at speed=5500 rpm and depth of cut =3.0 mm	160
4.35	SEM micrographs of uncoated tungsten carbide insert for conventional MQL after machining at depth of cut = 3.0 mm, speed = 5300 rpm, feed rate = 318 mm/min	160
4.36	Comparison of tool damage in flooded and MQL machining conditions for uncoated tungsten carbide insert for conventional MQL	162
4.37	SEM micrographs of TiAlN coated carbide insert for conventional MQL at speed=5300 rpm, feed rate = 440 mm/min, MQL flow rate = 0.83 ml/min	164
4.38	SEM micrographs TiAlN coated carbide insert for conventional MQL speed=5400 rpm, feed rate = 379 mm/min, MQL flow rate = 0.65 ml/min	166
4.39	SEM micrographs of TiAlN coated carbide insert for conventional MQL depth of cut = 2.0 mm	167
4.40	SEM images of TiAlN coated carbide insert for conventional MQL at speed = 5500 rpm	169
4.41	SEM micrographs of TiAlN coated carbide insert after machining at depth of cut = 3.0 mm, speed = 5300 RPM, feed rate = 318 mm/min	169
4.42	Comparison of tool damage in flooded and MQL machining conditions for Tool coated with TiAlN	171
4.43	SEM micrographs of TiAlN+TiN coated carbide insert for conventional MQL at speed=5300 rpm, feed rate = 440 mm/min, MQL flow rate = 0.83 ml/min	173

Figure No.	Title	Page
4.44	SEM micrographs of TiAlN+TiN coated carbide insert for conventional MQL at speed=5400 rpm, feed rate = 379 mm/min, MQL flow rate = 0.65 ml/min	174
4.45	SEM micrographs of TiAlN+TiN coated carbide insert for conventional MQL with depth of cut = 2.0 mm	177
4.46	SEM micrographs of TiAlN+TiN coated carbide insert for conventional MQL at speed=5500 rpm	179
4.47	SEM micrographs of TiAlN+TiN coated carbide insert for conventional MQL after machining at depth of cut = 3.0 mm, speed = 5300 rpm, feed rate = 318 mm/min	180
4.48	Comparison of catastrophic tool damage in flooded and MQL machining conditions for TiAlN+TiN coated insert in conventional MQL	181
4.49	EDX spectrums for unused tools	184
4.51	EDX spectrums of tools for Set -1 in conventional MQL conditions	185
4.52	EDX spectrums of tools for set -2 in conventional MQL conditions	186
4.53	SEM micrographs and EDX patterns for the machining condition with speed = 5400 rpm, feed rate = 370 mm/min, depth of cut = 2.25 mm, MQL flow rate = 0.65 ml/min, nanofluid-volume fraction = 0.5%	188
4.54	SEM micrographs and EDX patterns for the machining condition with speed = 5300 rpm, feed rate = 300 mm/min, depth of cut = 3.0 mm, MQL flow rate = 0.48 ml/min, nanofluid-volume fraction = 1.5%	189
4.55	SEM micrographs and EDX patterns for the machining condition with speed = 5300 rpm, feed rate = 440 mm/min, depth of cut = 3.0 mm, MQL flow rate = 0.83 ml/min, nanofluid-volume fraction = 1.5%.	191
4.57	SEM and EDX patterns for the machining conditions with speed = 5500 rpm, feed rate = 440 mm/min, depth of cut = 1.5 mm, MQL flow rate = 0.83 ml/min, nanofluid-volume fraction = 1.5%	195
4.58	SEM micrographs and EDX patterns for the machining condition with speed = 5500 rpm, feed rate = 440 mm/min, depth of cut = 1.5 mm, MQL flow rate = 0.48 ml/min, nanofluid-volume fraction = 3.5%	197

Figure No.	Title	Page
4.59	SEM micrographs and EDX patterns for the machining condition with speed = 5500 rpm, feed rate = 300 mm/min, depth of cut = 3.0 mm, MQL flow rate = 0.48 ml/min, nanofluid-volume fraction = 3.5%	199
4.60	SEM micrographs and EDS patterns for the machining condition with speed = 5500 RPM, feed rate = 440 mm/min, depth of cut = 3.0 mm, MQL flow rate = 0.48 ml/min, nanofluid-volume fraction = 1.5%	200
4.61	SEM micrographs and EDX patterns for the machining condition with speed = 5200 rpm, feed rate = 370 mm/min, depth of cut = 2.25 mm, MQL flow rate = 0.65 ml/min, nanofluid-volume fraction = 2.5%	201
4.62	SEM micrographs and EDX patterns for the machining condition with speed = 5600 rpm, feed rate = 370 mm/min, depth of cut = 2.25 mm, MQL flow rate = 0.65 ml/min, nanofluid-volume fraction = 2.5%	203
4.63	SEM micrographs and EDX patterns for the machining condition with speed = 5400 rpm, feed rate = 510 mm/min, depth of cut = 2.25 mm, MQL flow rate = 0.65 ml/min, nanofluid-volume fraction = 2.5%	205
4.64	SEM micrographs and EDX patterns for the machining condition with speed = 5400 rpm, feed rate = 370 mm/min, depth of cut = 2.25 mm, MQL flow rate = 0.65 ml/min, nanofluid-volume fraction = 4.5%	207
4.65	SEM micrographs and EDX patterns for the machining condition with speed = 5400 rpm, feed rate = 370 mm/min, depth of cut = 2.25 mm, MQL flow rate = 1.0 ml/min, nanofluid-volume fraction = 2.5%	208
4.67	SEM micrographs and EDX patterns for the machining condition with feed rate = 370 mm/min, depth of cut = 3.75 mm, MQL flow rate = 0.65 ml/min, nanofluid volume fraction = 2.5%	212
4.68	Deepest dimension extending into the tool body for determining volumetric flank wear of uncoated tungsten carbide insert in conventional MQL and nanofluid-MQL machining	219
4.69	Deepest dimension extending into the tool body for determining volumetric flank wear of TiAlN and TiAlN+TiN coated inserts in conventional MQL machining	220

Figure No.	Title	Page
4.70	Bubble chart showing Pareto designs distribution with input parameters for uncoated tungsten carbide insert in conventional MQL machining	222
4.71	Bubble chart showing Pareto designs distribution with input paramters for TiAlN coated carbide insert in conventional MQL machining	223
4.72	Bubble chart showing Pareto designs distribution with depth of cut for TiAlN+TiN coated carbide insert in conventional MQL machining	225
4.73	Bubble chart showing Pareto designs distribution with input parameters for uncoated tungsten carbide insert in nanofluid-MQL machining	226
4.74	Flank wear obtained from confirmation runs for conventional MQL and nanofluid-MQL conditions	230

LIST OF SYMBOLS

Symbol	Description
A_0, β_0, C_0	Constant
A_i, A_{ii}, A_{ij}	Regression coefficient
AISI 1040	A type of steel alloy
Al_2O_3	Aluminium oxide
B_i, B_{ii}, B_{ij}	Regression coefficient
β_i, β_{ij}, β_{ii}	Regression coefficient
BCBN	Binder-less Cubic Boron Nitride
C_i, C_{ii}, C_{ij}	Regression coefficient
CBN	Cubic Boron Nitride
Co	Cobalt
C45	A type of steel alloy
CuO	Copper oxide
CNT	Carbon nanotube
ε	Experimental error
f	Function
F-ratio	Fisher distribution
HAAS	HAAS Automation, Inc.
K20	Tool grade
k	Thermal conductivity
MSR-10D	Type of Tribotest
L_c	Tool extent

Symbol	Description
mm	Millimeter
min	Minute
MOGA-II	Multi-Objective Genetic Algorithm (II)
NiTi	Nickel-Titanium alloy
NAK80	40 HRC pre-Hardened, high performance, high precision, mold steel
PCD	Polycrystalline Diamond
PCBN	Polycrystalline Boron Nitride
ρ	Density
R_a	Average roughness parameter
R^2	Coefficient of Determination
SiO_2	Silicon dioxide
t	Time
T6	A type of heat treatment
TiAlN	Titanium Aluminium Nitride
TiN	Titanium Nitride
Ti6A14V	A type of Titanium-Aluminium-Vanadium alloy
TiO_2	Titanium dioxide
TNT	Titanate tubes
UNS S34700	Grade 347 austenitic stainless steel
VDI-3198	Hardness test method
WC	Tungsten carbide
wt %	Weight %
ZnO	Zinc oxide

Symbol	Description
x_{max}	Maximum value of the variable
x_{min}	Minimum value of the variable
y	Response
42CrMo4	A type of soft steel

LIST OF ABBREVIATIONS

AA	Aluminum alloy
ANOVA	Analysis of Variances
ASME	American Society for Mechanical Engineers
BUE	Built Up Edge
CCD	Central composite design
CNC	Computer Numerical Control
DLC	Diamond-like-carbon
DOE	Design of experiment
FESEM	Field Emission Scanning Electron Microscope
FW	Flank Wear
G-ratio	Grinding ratio
HPJAM	High Pressure Jet-Assisted Machining
HPC	High Pressure Coolants
ISO	International Standards Organization
MCDM	Multi-Criteria Decision Making
MQL	Minimum quantity lubrication
MWF	Metal working fluids
MVO	Minimum volume of oil
MRR	Material Removal Rate
M-ratio	Machining Ratio
NACFAM	National Council for Advanced Manufacturing
NIOSH	National Institute for Occupational Safety and Health
PVD	Physical vapor deposition

rpm	Revolutions per minute
RSM	Response surface methodology
SAE	Society of Automotive Engineers
SEM	Scanning Electron Microscope
SR	Surface Roughness
TEM	Transmission Electron Microscope
UHPC	Ultra-High Pressure Cooling

CHAPTER 1

INTRODUCTION

1.1 INTRODUCTION

Minimum quantity lubrication (MQL) refers to the application of a miniscule quantity of coolant, typically of a flow rate of 10 to 100 ml/hour (Kamata and Obikawa, 2007). Reducing the environmental impacts of machining are required in order to attain the sustainable and cleaner production. As developing alternative manufacturing process technologies for machining is still a prohibitive task, preventing the negative environmental impact of machining can be achieved essentially by operating modification of existing processes (Hanafi et al., 2012). As the manufacturing world is in a continuous pursuit of investigating the methods in order to increase the process performance and to reduce the production costs, in addition to the growing environmental concerns (Fratila, 2013), minimum quantity lubrication process can offer the near-term solution to the problem. Driven by pressure from international environmental protection agencies, energy consumption and natural resources conservation laws enforced by public authorities, manufacturing industry and the concerned research centers are forced to focus their efforts on researching alternative production processes, creating technologies to minimize the use and production of environmentally hostile residues. MQL has demonstrated as a successful near-dry machining technique as well as a globally-acknowledged option compared to complete dry and wet cutting conditions from the perspective of cost, ecological, human health issues and machining process performance (Lawal et al., 2013). MQL is a sustainable manufacturing approach which is vital in the current scenario of manufacturing industry as it incorporates all the issues related to sustainability. The cost of cutting fluids range from 7 to 17% of the total machining cost while another estimate gives this cost as 15-20 % of total machining cost compared to the tool cost which ranges from 2 to 4% (Attanasio et al., 2006; Lawal et al., 2013; Li et al., 2014). Therefore, the minimization of metal working fluids can serve as a direct gauge of sustainable manufacturing.

Machining with MQL has been extensively applied in many machining processes such as drilling (Filipovic and Stephenson, 2006; Davim et al., 2007), milling (Lacalle et al., 2006; Liao and Lin, 2007), turning (Davim, 2007; Kamata and Obikawa, 2007) and MQL grinding (Silva et al., 2005; Shen et al., 2008). Since no huge power consuming auxiliary equipment such as compressors, chillers and pumps are required as compared to flooded machining, hence a marked reduction in energy consumption in MQL machining. The use of empirical approach together with the implementation of experimental design techniques as well as application of statistical data analysis techniques are gaining recognition on account of the simplicity involved in the model making procedure and the accuracy of the prediction obtained for the specific cutting conditions domain (Kannan and Baskar, 2013).

Aluminium alloys are the most machinable amongst the metals with a wide range of applications due to mechanical and corrosion resistance with lower cutting forces as well as low cutting temperatures (Kelly and Cotterell, 2002; Ariff et al., 2012). However, due to highly adhesive characteristics of aluminium and its alloys more effective lubrication is required for these alloys although these are not hard and difficult-to-cut especially with alloys containing hard inclusions such as aluminium oxide, silicon carbide, or free silicon (Kelly and Cotterell, 2002; Wakabayashi et al., 2007). On the other hand, machining of aluminium alloys results in the generation of very fine metallic particles in the form of ultrafine dust particles with longer air-borne suspension time hence harmful for the health of the operator (Songmene et al., 2011).

Significance of machining processes optimization arises from the prerequisite for an economic and feasible performance of the machining processes. Practical manufacturing processes are illustrated by conflicting and often incompatible measures of performance such as quality and productivity (Kumar and Chhabra, 2014). The multi-objective optimization techniques are used to find out the trade-offs among the conflicting performance measures in a machining process in order to achieve performance

CHAPTER 1

INTRODUCTION

1.1 INTRODUCTION

Minimum quantity lubrication (MQL) refers to the application of a miniscule quantity of coolant, typically of a flow rate of 10 to 100 ml/hour (Kamata and Obikawa, 2007). Reducing the environmental impacts of machining are required in order to attain the sustainable and cleaner production. As developing alternative manufacturing process technologies for machining is still a prohibitive task, preventing the negative environmental impact of machining can be achieved essentially by operating modification of existing processes (Hanafi et al., 2012). As the manufacturing world is in a continuous pursuit of investigating the methods in order to increase the process performance and to reduce the production costs, in addition to the growing environmental concerns (Fratila, 2013), minimum quantity lubrication process can offer the near-term solution to the problem. Driven by pressure from international environmental protection agencies, energy consumption and natural resources conservation laws enforced by public authorities, manufacturing industry and the concerned research centers are forced to focus their efforts on researching alternative production processes, creating technologies to minimize the use and production of environmentally hostile residues. MQL has demonstrated as a successful near-dry machining technique as well as a globally-acknowledged option compared to complete dry and wet cutting conditions from the perspective of cost, ecological, human health issues and machining process performance (Lawal et al., 2013). MQL is a sustainable manufacturing approach which is vital in the current scenario of manufacturing industry as it incorporates all the issues related to sustainability. The cost of cutting fluids range from 7 to 17% of the total machining cost while another estimate gives this cost as 15-20 % of total machining cost compared to the tool cost which ranges from 2 to 4% (Attanasio et al., 2006; Lawal et al., 2013; Li et al., 2014). Therefore, the minimization of metal working fluids can serve as a direct gauge of sustainable manufacturing.

Machining with MQL has been extensively applied in many machining processes such as drilling (Filipovic and Stephenson, 2006; Davim et al., 2007), milling (Lacalle et al., 2006; Liao and Lin, 2007), turning (Davim, 2007; Kamata and Obikawa, 2007) and MQL grinding (Silva et al., 2005; Shen et al., 2008). Since no huge power consuming auxiliary equipment such as compressors, chillers and pumps are required as compared to flooded machining, hence a marked reduction in energy consumption in MQL machining. The use of empirical approach together with the implementation of experimental design techniques as well as application of statistical data analysis techniques are gaining recognition on account of the simplicity involved in the model making procedure and the accuracy of the prediction obtained for the specific cutting conditions domain (Kannan and Baskar, 2013).

Aluminium alloys are the most machinable amongst the metals with a wide range of applications due to mechanical and corrosion resistance with lower cutting forces as well as low cutting temperatures (Kelly and Cotterell, 2002; Ariff et al., 2012). However, due to highly adhesive characteristics of aluminium and its alloys more effective lubrication is required for these alloys although these are not hard and difficult-to-cut especially with alloys containing hard inclusions such as aluminium oxide, silicon carbide, or free silicon (Kelly and Cotterell, 2002; Wakabayashi et al., 2007). On the other hand, machining of aluminium alloys results in the generation of very fine metallic particles in the form of ultrafine dust particles with longer air-borne suspension time hence harmful for the health of the operator (Songmene et al., 2011).

Significance of machining processes optimization arises from the prerequisite for an economic and feasible performance of the machining processes. Practical manufacturing processes are illustrated by conflicting and often incompatible measures of performance such as quality and productivity (Kumar and Chhabra, 2014). The multi-objective optimization techniques are used to find out the trade-offs among the conflicting performance measures in a machining process in order to achieve performance optimization. In such cases, it is not necessary that a single solution may satisfy all the objectives on account of incommensurability and the conflict among the objectives. Multi-objective optimization is different from single objective optimization in that the single objective optimization is used to find the best design from among many and usually best design point is the global maximum or minimum depending on the type of optimization (Ponnala and Murthy, 2012). The investigations carried out in this study are focused on the effects, analysis and parametric modeling of end milling process under conventional minimum quantity lubrication technique through extensive experimentation as well as nanofluid-MQL conditions. Multi-objective optimization is performed in terms of desired performance measures within the defined machining domain.

1.2 PROBLEM STATEMENT

The major challenges faced by the manufacturing industry are the improved quality, enhanced productivity as well as economic production. These challenges are addressed by increasing the material removal rate for enhanced productivity, surface quality and surface integrity as well as longer tool life with consistence performance (Ali et al., 2011). While dealing with these issues, one of the predominating challenges is the mitigation of excessive heat generated in the cutting zone. This generated heat in the cutting zone affects surface quality and integrity as well as tool wear and tool life. Hence it is essential to maintain this cutting temperature at such an optimum level so as to attain superior surface finish and overall machining economy in terms of longer tool life and productivity. Cutting fluids are considered essential for machining operations in order to perform lubrication, cooling and chip flushing. These functions of cutting fluids in machining processes are constantly being reviewed due to cost pressures (Priarone et al., 2014) together with growing global concerns related to occupational and environmental consciousness (Marksberry and Jawahir, 2008) and the need for increased employee satisfaction through healthier environment and cleaner work areas (Ali et al., 2011). The conventional method of application of cooling and lubrication in machining processes involve profuse use of cutting fluids.

Consumption of cutting fluids in the different machining and technological processes often generates aerosols by atomization and the mist thus produced in the work area poses a potential exposure hazard to workers and to the environment (Sujova, 2012).

CHAPTER 3

EXPERIMENTAL WORK AND OPTIMIZATION MODELLING

3.1 INTRODUCTION

This chapter presents the details of experimental work as well as methodology adopted for modelling and multi-objective optimization. The selected materials and machining parameters (process parameters and performance parameters) are also presented. The preparations of TiO_2 nanofluid and properties determination are described. The application of response surface methodology for developing mathematical models and analysis of variances are explored. The subsequent sections of the chapter are laid out to include the design of experiments and the experimental setup, including the methods of performance's measurement. Multi-objective optimization technique used for data analysis is described in detail.

3.2 FLOWCHART OF THE STUDY

The flowchart of the study for the experimental set up, machining and analysis is presented in Figure 3.1. This flowchart shows a plan of experimental and analytical activities for different machining conditions. These activities include machine and equipment set-up, end milling machining experiments, preparation and use of nanofluids, measurements of machining performance parameters, analysis of experimental results, modelling and multi-objective optimization.

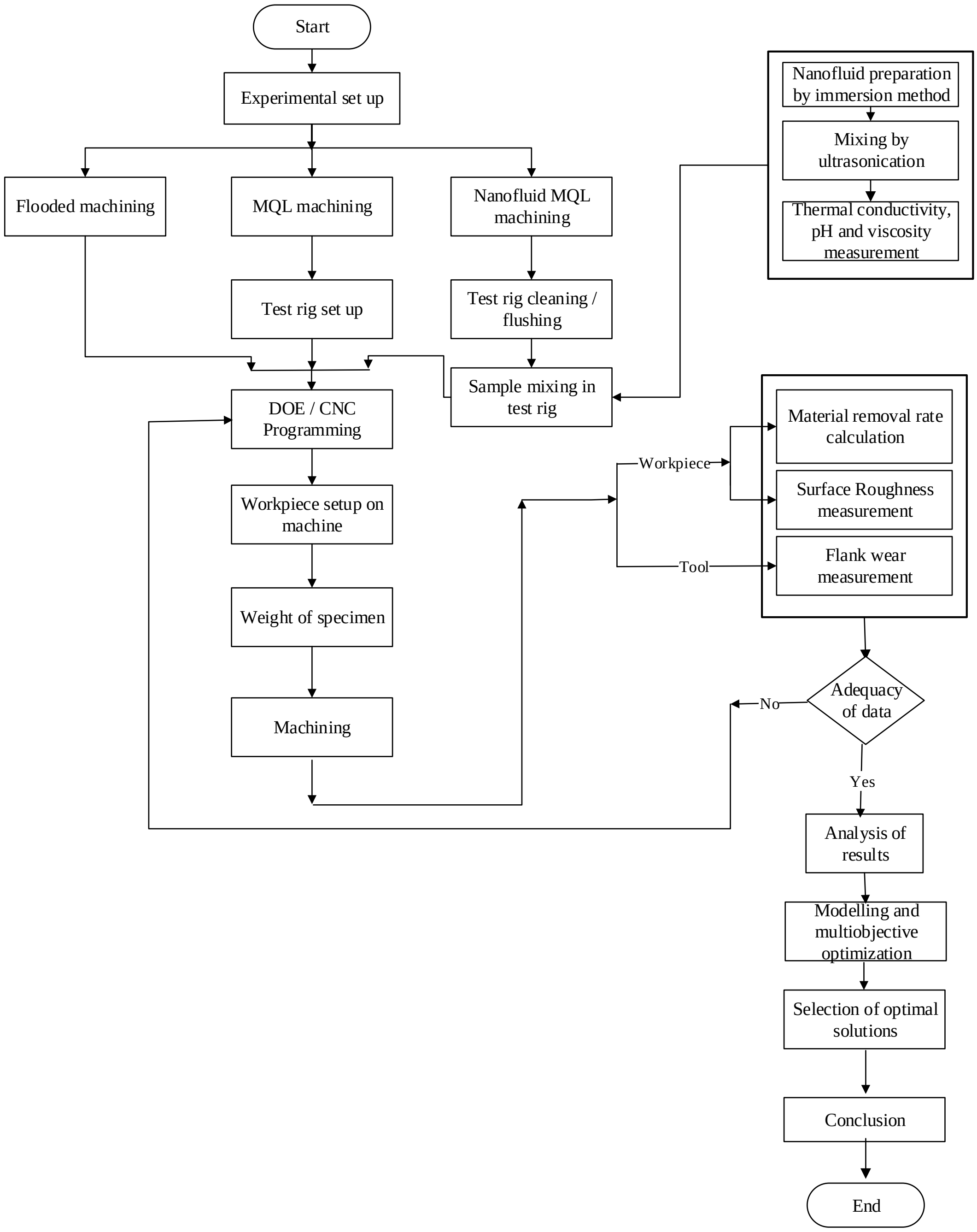

Figure 3.1: Flowchart of the study

3.3 MATERIALS

3.3.1 Workpiece Material

Aluminium alloy AA6061-T6 is selected as a workpiece material due to excellent mechanical properties and corrosion resistance (Rahmati et al., 2014). Conflicting views about the cooling conditions for the alloy are observed in literature

(Tosun and Huseyinoglu, 2010; Ariff et al., 2013). The alloy compositions as well as physical, mechanical and thermal properties are listed in Table 3.1 and Table 3.2. Hardness of the workpiece material is 107 HV while modulus of elasticity and ultimate tensile strength are 68.9 GPa and 310 MPa, respectively. Density of the workpiece material is measured as 2712 kg/m^3. The measured alloy composition conforms to the composition of the AA6061-T6 i.e. aluminium as well as the alloying elements are within the recommended range of ASM standard composition (ASM, 1990). Workpiece dimensions are 100 × 100 × 30 mm (Figure 3.2). Alloy composition is recorded using a spectrometer (Foundary-Master type, Oxford Instruments, Inc.) for three random samples at three different places each and weight % obtained is average of the nine samples. Slot machining is performed to obtain the experimental data on the workpiece. Machining slot features are considered difficult due to the full engagement of the cutting tool with the workpiece material (Dhokia et al., 2012). Blank workpiece, machined workpiece as well as machining pattern on a single workpiece is shown in Figure 3.2.

Table 3.1: The alloy composition of AA6061-T6.

Component (wt %)	Al	Si	Mn	Mg	Ti	Zn	Fe	Balance
Measured	97.6	0.71	0.13	0.8	0.03	0.05	0.25	Cr, V, Cu, Others
ASM (ASM, 1990)	95.8-98.6	0.4-0.8	Max. 0.15	0.8-1.2	Max. 0.15	Max. 0.25	Max. 0.7	Cr, Cu, Others

Table 3.2: Physical, thermal and mechanical properties of AA6061-T6.

Properties	Value	Properties	Value
Hardness, vickers	107	Density, kg/m^3	2712
Modulus of elasticity (GPa)	68.9	Melting point, °C	582
Ultimate tensile strength (MPa)	310	Fracture toughness (MPa-m$^{1/2}$)	29
Tensile yield strength (MPa)	276	Machinability, %	50
Elongation at break, %	17	Shear strength (GPa)	207
Thermal conductivity, W/m-K	167	Specific heat capacity, J/g-°C	0.896

3.3.2 Cutting Fluids

Three cutting environments including flooded (wet) cooling, conventional (oil-based) MQL and water-based nanofluid-MQL conditions are considered in the study.